FEBS Letters 583 (2009) 2833–2838

FEBS Letters

journal homepage: www.FEBSLetters.org

Channel-like NH_3 flux by ammonium transporter AtAMT2

Benjamin Neuhäuser [a], Marek Dynowski [a], Uwe Ludewig [a,b,*]

[a] Zentrum für Molekularbiologie der Pflanzen (ZMBP), Pflanzenphysiologie, Universität Tübingen, Auf der Morgenstelle 1, D-72076 Tübingen, Germany
[b] Applied Plant Sciences, Institute of Botany, Darmstadt University of Technology, Schnittspahnstr. 10, D-64287 Darmstadt, Germany

ARTICLE INFO

Article history:
Received 19 June 2009
Accepted 1 July 2009
Available online 25 July 2009

Edited by Julian Schroeder

Keywords:
Methylamine
Methylammonium
Gas channel
H^+-coupling

ABSTRACT

Prokaryotes, plants and animals control ammonium fluxes by the regulated expression of ammonium transporters (AMTs) and/or the related Rhesus (Rh) proteins. Plant AMTs were previously reported to mediate electrogenic transport. Functional analysis of AtAMT2 from Arabidopsis in yeast and oocytes suggests that NH_4^+ is the recruited substrate, but the uncharged form NH_3 is conducted. AtAMT2 partially co-localized with electrogenic AMTs and conducted methylamine with low affinity. This transport mechanism may apply to other plant ammonium transporters and explains the different capacities of AMTs to accumulate ammonium in the plant cell.

1. Introduction

Ammonium (this term designates the sum of NH_4^+ and NH_3) is an important nutrient and ubiquitous intermediate in nitrogen metabolism. Its transport and distribution across cellular membranes depends on AMT/Rh ammonium transporters [1,2]. In plants and microorganisms, the AMT/Rh-mediated ammonium transport is critical for providing sufficient nitrogen for optimal growth [1,2].

The crystal structures of several AMT/Rhs, including AmtB from *Escherichia coli*, showed that these proteins are arranged as (homo-) trimers and each subunit forms a hydrophobic pore in its center [3–5]. There is compelling evidence that NH_4^+ is recruited by AMT/Rhs at the external pore entrance, but the structures suggested that the ion is de-protonated, and NH_3 passes the channel [3–5]. This mechanism is supported by molecular simulation studies on EcAmtB, although the site of de-protonation is disputed [6–8]. A central phenylalanine has recently been experimentally determined to be critical [9]. Although some functional evidence supports this mechanism [3], several studies questioned whether "equilibrative" NH_3 transfer occurs in EcAmtB [9–11]. The structurally related plant AMT1s, in contrast, function as net transporters for NH_4^+ [12–16].

In the model plant *Arabidopsis*, three ammonium transporters (AtAMT1;1, AtAMT1;2 and AtAMT1;3) were responsible for ~90% of the total high affinity uptake in roots [17]. The more distant AtAMT2 was also expressed in roots, but did not contribute to the uptake [17,18]. In general, the molecular function and physiological role of plant AMT2 proteins is much less evident than those of AMT1s, although their potential relevance is highlighted by their abundance in plant genomes [1]. While *Arabidopsis* has only a single *AMT2* gene, other plants have multiple *AMT2* sequences in their genomes, e.g. rice has seven *AMT2*-like isoforms [1]. In this study, AtAMT2 was functionally analyzed in yeast and oocytes. The results suggest that AtAMT2 recruited NH_4^+, but mediated electroneutral ammonium transport, probably in the form of NH_3.

2. Materials and methods

2.1. Generation of constructs

The cDNA from *AtAMT2* (At2g38290) was amplified from a Landsberg cDNA library by PCR using Phusion polymerase (New England Biolabs, Ipswich, MA) with the following primers: AMT2-Fw: CAGGGATCCATGGCCGGAGCTTACGATCCAAG AMT2-Rv: GAGCTCGAGTCATAGAACAATGGTGACACCTCTAG. This and other PCR products were cloned into pCR-Blunt II-TOPO (Invitrogen) and were fully sequenced. The *AtAMT2* open reading frame was identical to the *AtAMT2* sequence from the *C24* ecotype (*AAF37192*) and contained two nucleotide exchanges compared to the *Col-0* sequence. The translated protein sequences differ at the non-conserved position 95: in *Col-0* that residue is aspartate, while in *C24* it is asparagine. Two independent clones confirmed that this amino acid exchange compared to *Col-0* did not result from a PCR error. The sequence was further subcloned into pOO2

* Corresponding author. Present address: Applied Plant Sciences, Institute of Botany, Darmstadt University of Technology, Schnittspahnstr. 10, D-64287 Darmstadt, Germany. Fax: +49 7071 29 3287.
E-mail address: ludewig@bio.tu-darmstadt.de (U. Ludewig).

0014-5793/$36.00
doi:10.1016/j.febslet.2009.07.039

(oocyte) and pDR199 (yeast) expression vectors using the BamHI and XhoI sites.

The 1.7 kB promoter fragment 5′ upstream of the *ATG* of *AtAMT2* was amplified from genomic *Arabidopsis* (ecotype *Col-0*) DNA using the forward primer AMT2-Prom-Fw: GAGAGGTACCAATGATTCGATCTTTTGTCTTCTCATAG and the reverse primer AMT2-Pr-Rv: CTTGGATCGTAAGCTCCGGCCATTTTGTTATTC. By a recombinant PCR of the *AtAMT2* ORF and the promoter fragment with the primers AMT2-Prom-Fw and AMT2-GFP-Rv: GAGATCTAGATAGAACAATGGTGACACCTCTAGCAC, a 3.1 kB *pAMT2:AtAMT2* fragment was obtained. This was cloned into *pCR-BluntII-TOPO*, sequenced and subcloned into the plant transformation binary vector *pTkan^{+}GFP* using the KpnI and XbaI restriction sites. The reverse primer was designed to eliminate the STOP codon and to generate a translational fusion with GFP.

2.2. Plant growth and analysis

Arabidopsis thaliana plants (ecotype *Col-0*) were grown in soil and transformed using the GV3101 agrobacterium strain by spraying. Transgenic plant selection and segregation for kanamycin resistance analysis to achieve homogeneity was performed on MS plates containing 1X Murashige and Skoog salt (Duchefa), 1% sucrose, 0.8% agar and 50 μg/ml kanamycin. 6 to 30-day old fluorescent plants, grown on standard medium (0.8% Agar, 1 mM KH_2PO_4, 0.5 mM $MgSO_4$, 100 μM $NaSiO_3$, 1.25 mM $CaSO_4$, 50 μM Na–Fe–EDTA, 50 μM H_3BO_3, 3 μM $MnSO_4$, 1 μM $ZnSO_4$, 1,3 μM $CuSO_4$, 0,03 μM $Mo_7O_{24}(NH_4)_6$ and 20 mM MES, with the pH adjusted to 6.0 using Tris) supplemented with 0–200 μM NH_4NO_3 as nitrogen source were analyzed by a Leica confocal microscope (Wetzlar, Germany) using the 488 nm Ar laser excitation beam line and a 505–530 nm band pass filter.

2.3. Yeast transformation

The plasmids containing the respective open reading frames were heat shock-transformed in the *ura*$^{-}$ wild type (23344c), and the *ura*$^{-}$ ammonium transporter defective yeast strain (31019b; *triple-Δmep*) [19]. Selection for transformed yeast was done on solid arginine medium (2% Agar, 0.17% YNB w/o amino acids and ammonium sulfate (Difco), supplemented with 3% glucose and 0.1% arginine (Arg) as nitrogen source, buffered with 20 mM MES/Tris, pH 6.1.

2.4. Yeast growth assays

Yeast was grown in liquid Arg medium until OD_{595} (optical density at 595 nm) reached 0.6–0.8. Cells were harvested, washed and resuspended in water to a final OD_{595} of 2. 10 μl of OD_{595} 2 cells and 5-fold dilutions were spotted on Arg medium with or without MeA (pH 6.0), or media containing no Arg, but 1 mM NH_4Cl as sole nitrogen source, as well as 10 mM $MgCl_2$ and 100 mM KCl.

2.5. Yeast uptake

Yeast was grown in liquid arginine medium until the OD_{595} reached 0.6–0.8. Cells were harvested, washed and resuspended in uptake buffer (50 mM potassium phosphate buffer supplemented with 0.6 M sorbitol, pH 6) to a final OD_{595} of 5. Before the uptake, cells from the data shown were energized by adding 10 μl of 1 M glucose to 100 μl cells OD_{595} 5 and incubated for 7 min at 30 °C. As controls, uptakes were also done with non-energized cells (by adding 10 μl uptake buffer and incubation), which gave qualitatively the same results. The uptake was started by adding 110 μl of uptake buffer containing ^{14}C-MeA (2.11 Gbq/mmol, Amersham Bioscience). 50 μl samples were taken after 30, 60, 120 and 300 s and washed three times in 4 ml ice-cold washing solution (uptake buffer containing a 100-fold excess of non-labled MeA). Immediately after taking the sample, the solution was filtered through glass fiber filters (GF/C, Whatman). The filters containing the yeast were measured by a liquid scintillation counter.

2.6. Electrophysiological measurements, preparation and injection of oocytes

These methods have been described in more detail elsewhere [20]. Briefly, oocytes were taken from adult females, dissociated by collagenase treatment (2 μg/ml, 1.5 h) and injected with 50 nl of cRNA (1 ng/nl). Oocytes were kept in ND96 for 3 days at 16 °C and then placed in a small recording chamber containing the recording solution (in mM): 110 CholineCl, 2 $CaCl_2$, 2 $MgCl_2$, 5 N-morpholinoethane sulfonate (MES), pH adjusted to 6.0 with tris(hydroxymethyl) aminomethane (TRIS). Ammonium and methylammonium (MeA) were added as Cl salts.

2.7. Homology modeling and display of plant AMTs

This was carried out using the MODELLER software package (version 9v3, http://salilab.org/modeller/modeller.html). The models were based on three high-resolution structures of EcAmtB (PDB ID: 1U7G, 1XQF, 2NS1) and the high-resolution structure of AfAmt-1 (PDB ID: 2B2H). 42 amino acids (AA) of the N-terminus and 33 AA of the C-terminus of the primary sequence of AtAMT1;2 were truncated. In AtAMT2, 13 AA of the N-terminus and 38 AA of the C-terminus of the primary sequence were removed. Multiple sequence alignments were performed using the clustalW method with standard parameters from MegAlign. The sequence alignments were inspected visually, minor adjustments were made and these were then used for homology modeling. Graphical representations were prepared using the software 'Pymol' (http://www.pymol.org).

3. Results

3.1. AtAMT2 partially co-localized with AtAMT1 transporters

AtAMT2 expression in roots has been reported, but AtAMT2 did not contribute to the ammonium uptake by the roots [17]. To resolve this discrepancy, the cell specificity of AtAMT2 expression was analyzed. The gene was tagged with green fluorescent protein and expressed from the endogenous promoter. The rhizodermal cells of lateral roots were labeled with AtAMT2-GFP, and a weaker expression in inner root tissues was observed (Fig. 1). AtAMT2 localized to the plasma membrane of the root hairs (Fig. 1). This expression in the plasma membrane of rhizodermal cells is shared by AtAMT1;1 and AtAMT1;3 [14,21]. In photosynthetic tissues, AtAMT2 expression was most significant in the pith of the stem, the petioles and leaf hydathodes (Supplementary Fig. S1). A slightly distinct pattern had been reported using a reporter construct with a shorter promoter [18]. The AtAMT2-GFP fluorescence was lower in roots than in shoots and was slightly up-regulated by nitrogen starvation, in accordance with the mRNA and protein levels [17].

3.2. AtAMT2 is functionally distinct from AtAMT1 transporters when expressed in yeast

Since the localization data conflicted the lack of AtAMT2 activity in roots, the transporter was expressed in yeast and further functionally characterized. In accordance with earlier data [18], AtAMT2 improved the growth of a yeast strain lacking endogenous ammonium transporters (*triple-Δmep*) on selective media (Fig. 2A).

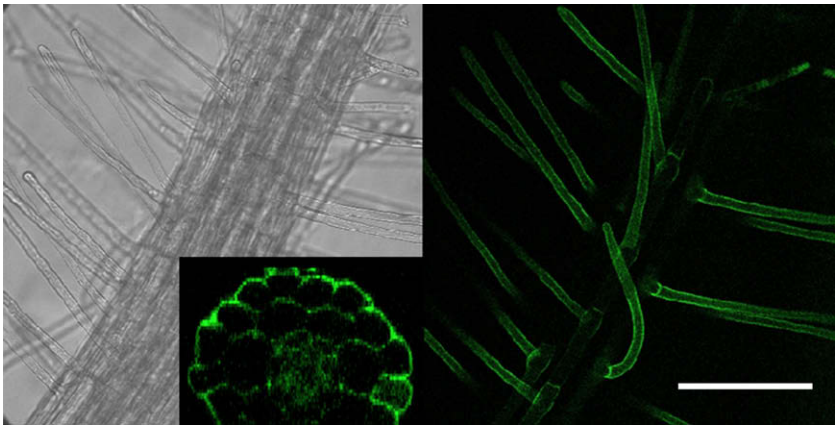

Fig. 1. Localization of AtAMT2 in lateral roots and root hairs. Bright field image (left) and AtAMT2-GFP fluorescence (green, right) of the same lateral roots, including root hairs. The confocal slice was thinner than the bright field image, so that the fluorescence was restricted to those cells in focus. The inset shows a 2D reconstruction of a section across a lateral root. Scaling bar: 100 μm.

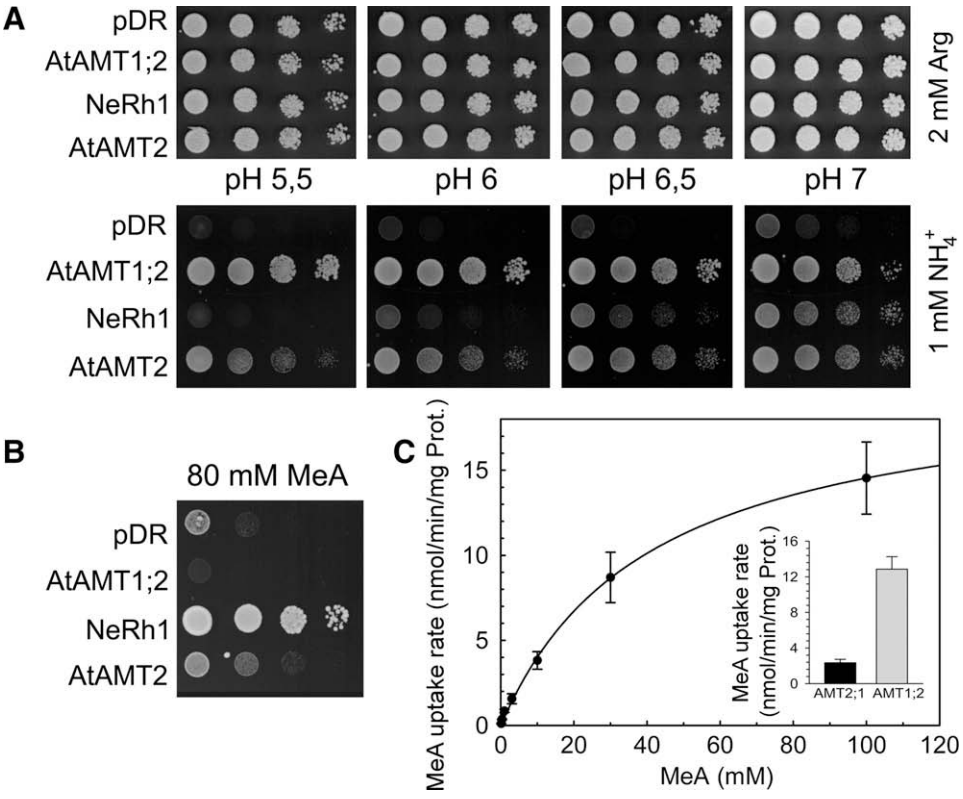

Fig. 2. Functional characteristics of AtAMT2 in yeast. (A) Growth of ammonium transporter-deficient yeast (*triple-Δmep*) transformed with control plasmid *pDR199*, *pDR199-AtAMT1;2*, *pDR199-NeRh-1* and *pDR199-AtAMT2* on control plates (2 mM arginine) or selective plates containing 1 mM NH_4^+ as sole nitrogen source. The pH of the media was adjusted to 5.5–7.0. Spotted 5-fold dilutions of cultures OD_{595} 2. (B) Growth of the wild type yeast strain transformed with the same constructs on 80 mM MeA. (C) Concentration-dependence of the ^{14}C-MeA uptake rate of AtAMT2 at pH 6.0 (S.D., $n = 4$). Inset: Background-subtracted (from vector control) ^{14}C-MeA uptake (100 μM) activity of AtAMT1;2 and AtAMT2 in yeast (S.D., $n = 4$).

This growth complementation was similar at acidic and neutral external pH (pH_{ext}). Since the concentration of NH_3 is about 30-fold lower at pH 5.5, compared to pH 7.0 and that of NH_4^+ remains almost constant, these data suggest that NH_4^+, rather than NH_3, is the substrate of AtAMT2. The same conclusion was obtained in previous study, as the half-maximal transport activity was close to ~20 μM NH_4^+, irrespective of pH_{ext} [18]. That NH_4^+ is the substrate of AtAMT2, however, does not necessarily mean that NH_4^+ is finally transported. Indeed, in bacterial AMTs NH_4^+ appears to be de-protonated before transport and conduction occurs as NH_3 [2–5].

Interestingly, AtAMT2 had been proposed to be impermeable for the toxic analog methylammonium and functionally differed in that respect from all other known AMT/Rhs [18,22]. Methylammonium (MeA) is used here to denote the sum of the charged and uncharged species; methylamine is specifically used for the uncharged weak base form. We observed that on MeA, wild type yeast expressing AtAMT2 showed a slightly improved growth compared to empty vector controls, similar to yeast that expressed bacterial NeRh-1 from *Nitrosomonas europaea* (Fig. 2B) [23]. This slightly enhanced resistance by AtAMT2 was opposite to the effect

of other plant AMTs, e.g. AtAMT1;2, which increased the sensitivity towards MeA (Fig. 2B). The different susceptibilities of NeRh-1 and AtAMT2-expressing cells to MeA, compared to AtAMT1;2, were also manifested in the *triple-Δmep* yeast (Supplementary Fig. S2). Interestingly, an improved growth on high MeA had been consistently observed with cells expressing various NH_3 channels, such as plant aquaporins [24] and Rh-homologs from humans [13,25,26], but not with NH_4^+ transporting AtAMT1s from plants [13].

MeA transport by AtAMT2 was confirmed by ^{14}C-MeA uptake assays in yeast. The uptake was more than doubled by AtAMT2 and increased at more alkaline pH_{ext}, which is in accordance with previous ^{13}N ammonium uptake studies [18]. Transport was half-maximal at 41 ± 3 mM (Fig. 2C). The MeA uptake rate of AtAMT1;2 was more than 7-fold larger (Fig. 2C, inset), which is consistent with the improved yeast growth by AtAMT1;2, compared to AtAMT2 (Fig. 2A).

3.3. The transport by AtAMT2 is electroneutral

AtAMT2 was then expressed and assayed in *Xenopus* oocytes using a combination of ^{14}C-MeA uptakes and two-electrode voltage clamp measurements. The AtAMT2-expressing oocytes imported ^{14}C-MeA (Fig. 3B), but MeA did not elicit any currents, even at very negative voltages (Fig. 3A and C). No currents were elicited by NH_4^+, as well. In contrast, AtAMT1;2-expressing oocytes imported similar amounts of ^{14}C-MeA and showed large MeA- and ammonium-dependent currents (Fig. 3). The combined data suggest that the transport by AtAMT2 was electroneutral, i.e. that the transported species across the membrane were NH_3 or methylamine. Taking into account the pH_{ext}-independence of the growth complementation (Fig. 2A) and of the K_m [18], these data suggest that AtAMT2 apparently recruits external NH_4^+, de-protonates the ion, and finally conducts NH_3, similar to other AMT/Rhs [3–5].

3.4. Structural models suggest a NH_4^+ recruitment site in AtAMT2

EcAmtB and NeRh-1 share a very similar structural fold, a hydrophobic pore and a putative de-protonation site around the phenylalanine gate [5]. They differ in the ion recruitment site, which is degenerated in Rhs [5]. Sequence comparisons and models suggest that the overall pore architecture is well preserved in AtAMT2 (Fig. 4). Most functionally important pore residues are identical to EcAmtB, except for the residues corresponding to serine 219 of EcAmtB, which is alanine in AtAMT2, and that corresponding to alanine 162, which is serine (Fig. 4). The external pore vestibule in AtAMT2 forms an aromatic NH_4^+ recruitment site, in accordance with the pH_{ext}-independence of the saturation constant [18] and the pH_{ext}-independent growth complementation of yeast by AtAMT2 (Fig. 2). The similarity of residues lining the EcAmtB and AtAMT2 pores, and their highly hydrophobic nature, support the idea that NH_3 is conducted.

4. Discussion

The high affinity ammonium transport in plants, which is mediated by AMTs [17], is classically viewed as NH_4^+ transport [1,2,12]. Using expression in oocytes, we showed that the ammonium fluxes

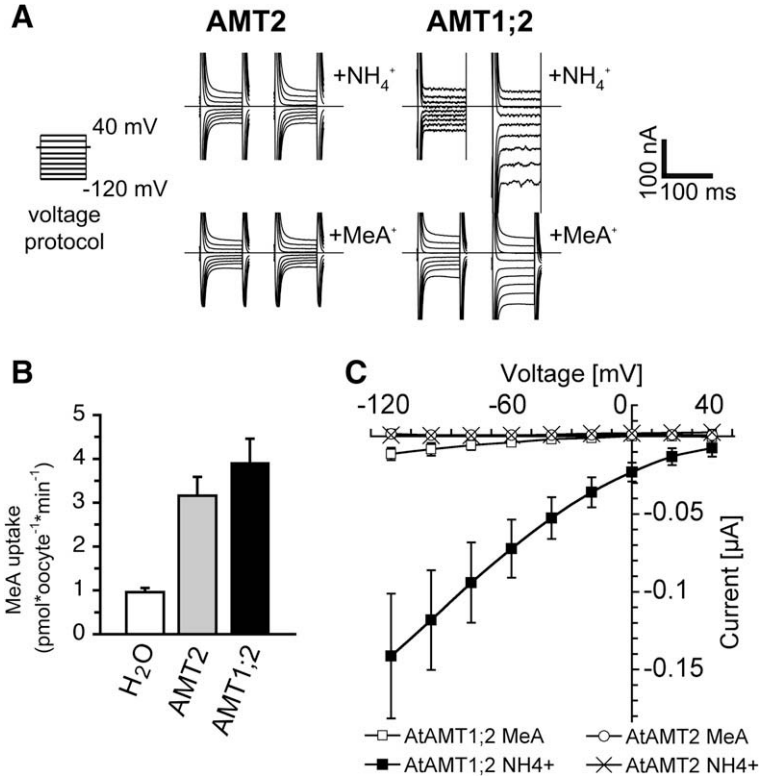

Fig. 3. Functional characteristics of AtAMT1;2 and AtAMT2 in *Xenopus* oocytes. (A) Original traces of ionic currents elicited by the voltage protocol shown at the left from 40 mV in −20 mV steps to −120 mV. Oocytes expressing AtAMT2 and AtAMT1;2 in the absence of ammonium (upper left) and in the presence of ammonium (1 mM) and with methylammonium (3 mM, lower panels). All currents were recorded at pH 6.0. (B) ^{14}C-MeA uptake (1 mM) in oocytes expressing AtAMT2 (S.E.M., $n = 8$, pooled data from independent measurements), AtAMT1;2 ($n = 3$) and controls. (C) Current–voltage plot of ammonium- and methylammonium-induced currents (each 1 mM; closed squares: AMT1;2 with NH_4^+; open squares: AMT1;2 with MeA; crosses: AMT2 with NH_4^+; open circles: AMT2 with MeA). All currents were recorded at pH 6.0 from the same batch of oocytes. Note that the MeA uptake activity of AtAMT1;2 vs. AtAMT2 was similar in oocytes, but a large difference was measured in yeast. This was likely due to the much more negative membrane potential of yeast, although we cannot exclude different expression levels of each transporter in both systems.

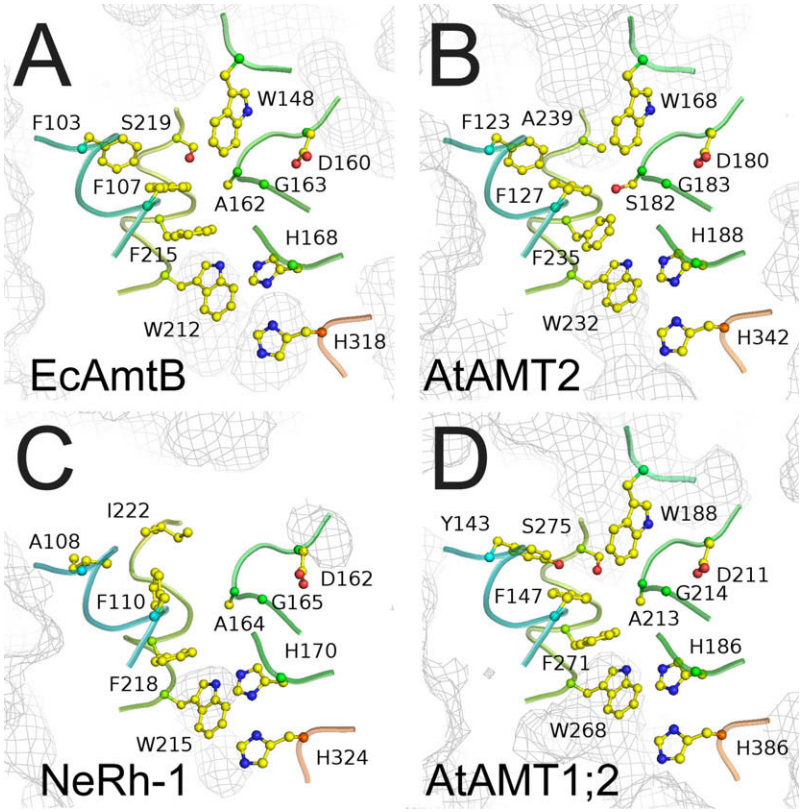

Fig. 4. Structural similarity of AMT/Rh pore structures and models. View into the pores of (A) EcAmtB (PDB code: 1U7G), (B) model of AtAMT2, (C) NeRh-1 (PDB code: 3B9 W), and (D) model of AtAMT1;2. Proposed residues involved in NH_4^+ recruitment, de-protonation and NH_3 conduction are explicitly shown. The water-accessible protein surface is shown as grey mesh.

by AtAMT2, in contrast, were electroneutral, which suggests that NH_3 was transported. Although the initial data from yeast are most consistent with the idea that NH_4^+ is the substrate of AtAMT2, the data from oocytes rule out that AtAMT2 is simply a channel for NH_4^+. On the other hand, the lack of ionic currents argues in favor of a NH_3 channel mechanism, but the pH_{ext}-independence from yeast growth argues against that. Indeed, the structural model of AtAMT2 supports a more complicated mechanism, which includes NH_4^+ recruitment and channel-like NH_3 conduction. That mechanism had been proposed for other AMTs [2–5]. However, structural models (and static structures) must be interpreted with much care. This is most obvious from the fact that the model of AtAMT1;2 also shows the hallmarks of AMT/Rhs (Fig. 4D), but the electrogenic transport mechanism in AtAMT1;2 differs from that in AtAMT2 (Fig. 3). AMT/Rhs generally lack potentially charged side chains in the transmembrane core, with the exception of a conserved and essential aspartate close to the external vestibule (D160 in EcAmtB). This residue is essential for function in several AMT/Rhs [27], but cannot account for isoform-specific differences.

Assuming that ammonium is conducted through a simple NH_3 pore, the transport activity should be proportional to the concentration of NH_3 and higher at alkaline pH_{ext}. Such a promotion of yeast growth at higher pH_{ext} has been observed with more genuine NH_3 channels, such as aquaporins [24] or Rh-homologs [13,25,26]. Furthermore, NeRh-1 improved growth on MeA, as did AtAMT2, but not AtAMT1;2 (Fig. 2B). This may argue in favor of some mechanistic similarities of NeRh-1 and AtAMT2, but the mechanism of MeA resistance (and toxicity) is likely to be complex and may involve efflux across the plasma membrane, pH effects [13,26] and MeA storage in intracellular compartments. Heterologously expressed AMTs were not exclusively localized to the yeast plasma membrane, but were also present at variable levels in non-identified intracellular structures [15,20,28].

The proposed transport mechanism offers an explanation why AtAMT2 did not significantly contribute to the uptake into well energized plant roots, compared to the voltage- and pH-gradient-driven electrogenic AMT1s [17]. Coupling of NH_3 to the proton gradient (as net NH_4^+ transport) is expected to enhance the uptake under most physiological conditions, but an electroneutral transport mechanism may be advantageous under certain conditions. For example, if uptake occurs as NH_3, the otherwise co-transported protons must not actively be exported by energy consuming H^+-pumps. Nevertheless, AtAMT2 contains a high affinity NH_4^+ recruitment site (Fig. 4B), and this may explain why that transporter was more effective in promoting yeast growth at low pH_{ext} than Rh proteins, which have lost such a high affinity site [5,23] (Fig. 4C).

The exact intracellular ammonium concentration in plants remains uncertain and a matter of discussion [29], but an outwardly directed NH_3 gradient is expected for many physiologic conditions. Whether AtAMT2 can mediate NH_3 efflux remains unknown, but a significant unexplained ammonium efflux occurs in various species [30].

The localization of AtAMT2 in the root hair zone of lateral roots suggests that it partially co-localized with functionally distinct AMT1 transporters [14,21]. The tissue specificity obtained here using a 1.7 kb promoter that extended to the neighboring gene was in accordance with northern analysis and transcript distribution from microarrays (Supplementary Fig. S1). However, this tissue distribution somewhat differed from the pattern deduced from a shorter 1 kb promoter-GUS reporter line [18], suggesting that the earlier construct lacked part of the true promoter. The simultaneous expression of AMT1 and AMT2 transporters in the

same cells is expected to lead to a proton leak, at least when the transport activity is not regulated by post-translational mechanisms. This may partially explain the high energy demand of NH_4^+-fed plants [30]. Recent analysis of a mycorrhiza-specific AMT2 from *Lotus japonicus* also suggested electroneutral NH_3 transport in that AMT, which may suggest that electroneutral NH_3 transport is realized in many, if not all, AMT2s [31].

Acknowledgements

We thank P. Neumann for excellent technical assistance, I. Schmidt for the NeRh-1 clone and F. de Courcy for critically reading the manuscript. This work was supported by grants of the Deutsche Forschungsgemeinschaft.

Appendix A. Supplementary data

Supplementary data associated with this article can be found, in the online version, at doi:10.1016/j.febslet.2009.07.039.

References

[1] Loque, D. and von Wiren, N. (2004) Regulatory levels for the transport of ammonium in plant roots. J. Exp. Bot. 55, 1293–1305.
[2] Ludewig, U. (2006) Ion transport versus gas conduction: function of AMT/Rh-type proteins. Transfus. Clin. Biol. 13, 111–116.
[3] Khademi, S., O'Connell 3rd, J., Remis, J., Robles-Colmenares, Y., Miercke, L.J. and Stroud, R.M. (2004) Mechanism of ammonia transport by Amt/MEP/Rh: structure of AmtB at 1.35 Å. Science 305, 1587–1594.
[4] Zheng, L., Kostrewa, D., Berneche, S., Winkler, F.K. and Li, X.D. (2004) The mechanism of ammonia transport based on the crystal structure of AmtB of *Escherichia coli*. Proc. Natl. Acad. Sci. USA 101, 17090–17095.
[5] Lupo, D., Li, X.D., Durand, A., Tomizaki, T., Cherif-Zahar, B., Matassi, G., Merrick, M. and Winkler, F.K. (2007) The 1.3-A resolution structure of Nitrosomonas europaea Rh50 and mechanistic implications for NH3 transport by Rhesus family proteins. Proc. Natl. Acad. Sci. USA 104, 19303–19308.
[6] Bostick, D.L. and Brooks 3rd, C.L. (2007) Deprotonation by dehydration: the origin of ammonium sensing in the AmtB channel. PLoS Comput. Biol. 3, e22.
[7] Nygaard, T.P., Rovira, C., Peters, G.H. and Jensen, M.O. (2006) Ammonium recruitment and ammonia transport by *E. coli* ammonia channel AmtB. Biophys. J. 91, 4401–4412.
[8] Luzhkov, V.B., Almlof, M., Nervall, M. and Aqvist, J. (2006) Computational study of the binding affinity and selectivity of the bacterial ammonium transporter AmtB. Biochemistry 45, 10807–10814.
[9] Javelle, A., Lupo, D., Ripoche, P., Fulford, T., Merrick, M. and Winkler, F.K. (2008) Substrate binding, deprotonation, and selectivity at the periplasmic entrance of the *Escherichia coli* ammonia channel AmtB. Proc. Natl. Acad. Sci. USA 105, 5040–5045.
[10] Javelle, A., Lupo, D., Li, X.D., Merrick, M., Chami, M., Ripoche, P. and Winkler, F.K. (2007) Structural and mechanistic aspects of Amt/Rh proteins. J. Struct. Biol. 158, 472–481.
[11] Fong, R.N., Kim, K.S., Yoshihara, C., Inwood, W.B. and Kustu, S. (2007) The W148L substitution in the *Escherichia coli* ammonium channel AmtB increases flux and indicates that the substrate is an ion. Proc. Natl. Acad. Sci. USA 104, 18706–18711.
[12] Ludewig, U., von Wirén, N. and Frommer, W.B. (2002) Uniport of NH_4^+ by the root hair plasma membrane ammonium transporter LeAMT1;1. J. Biol. Chem. 277, 13548–13555.
[13] Mayer, M., Schaaf, G., Mouro, I., Lopez, C., Colin, Y., Neumann, P., Cartron, J.P. and Ludewig, U. (2006) Different transport mechanism in plant and human AMT/Rh-type ammonium transporters. J. Gen Physiol. 127, 133–144.
[14] Mayer, M. and Ludewig, U. (2006) Role of AMT1;1 in NH_4^+-acquisition in Arabidopsis thaliana. Plant. Biol. (Stuttg) 8, 522–528.
[15] Neuhäuser, B., Dynowski, M., Mayer, M. and Ludewig, U. (2007) Regulation of NH_4^+ transport by essential cross-talk between AMT monomers trough the carboxyl-tails. Plant Physiol. 143, 1651–1659.
[16] Wood, C.C., Poree, F., Dreyer, I., Koehler, G.J. and Udvardi, M.K. (2006) Mechanisms of ammonium transport, accumulation, and retention in ooyctes and yeast cells expressing Arabidopsis AtAMT1;1. FEBS Lett. 580, 3931–3936.
[17] Yuan, L., Loque, D., Kojima, S., Rauch, S., Ishiyama, K., Inoue, E., Takahashi, H. and von Wiren, N. (2007) The organization of high-affinity ammonium uptake in arabidopsis roots depends on the spatial arrangement and biochemical properties of AMT1-type transporters. Plant Cell 19, 2636–2652.
[18] Sohlenkamp, C., Wood, C.C., Roeb, G.W. and Udvardi, M.K. (2002) Characterization of Arabidopsis AtAMT2, a high-affinity ammonium transporter of the plasma membrane. Plant Physiol. 130, 1788–1796.
[19] Marini, A.M., Soussi-Boudekou, S., Vissers, S. and André, B. (1997) A family of ammonium transporters in *Saccharomyces cerevisiae*. Mol. Cell. Biol. 17, 4282–4293.
[20] Mayer, M., Dynowski, M. and Ludewig, U. (2006) Ammonium ion transport by the AMT/Rh homolog LeAMT1;1. Biochem. J. 396, 431–437.
[21] Loque, D., Yuan, L., Kojima, S., Gojon, A., Wirth, J., Gazzarrini, S., Ishiyama, K., Takahashi, H. and von Wiren, N. (2006) Additive contribution of AMT1;1 and AMT1;3 to high-affinity ammonium uptake across the plasma membrane of nitrogen-deficient Arabidopsis roots. Plant J. 48, 522–534.
[22] Sohlenkamp, C., Shelden, M., Howitt, S. and Udvardi, M. (2000) Characterization of Arabidopsis AtAMT2, a novel ammonium transporter in plants. FEBS Lett. 467, 273–278.
[23] Weidinger, K., Neuhauser, B., Gilch, S., Ludewig, U., Meyer, O. and Schmidt, I. (2007) Functional and physiological evidence for a Rhesus-type ammonia transporter in Nitrosomonas europaea. FEMS Microbiol. Lett. 273, 260–267.
[24] Loqué, D., Ludewig, U., Yuan, L. and von Wiren, N. (2005) Tonoplast aquaporins AtTIP2;1 and AtTIP2;3 facilitate NH_3 transport into the vacuole. Plant Physiol. 137, 671–680.
[25] Marini, A.M., Matassi, G., Raynal, V., André, B., Cartron, J.P. and Cherif-Zahar, B. (2000) The human Rhesus-associated RhAG protein and a kidney homologue promote ammonium transport in yeast. Nat. Genet. 26, 341–344.
[26] Westhoff, C.M., Siegel, D.L., Burd, C.G. and Foskett, J.K. (2004) Mechanism of genetic complementation of ammonium transport in yeast by human erythrocyte Rh-associated glycoprotein (RhAG). J. Biol. Chem. 279, 17443–17448.
[27] Marini, A.M., Boeckstaens, M., Benjelloun, F., Cherif-Zahar, B. and Andre, B. (2006) Structural involvement in substrate recognition of an essential aspartate residue conserved in Mep/Amt and Rh-type ammonium transporters. Curr. Genet. 49, 364–374.
[28] Loque, D., Lalonde, S., Looger, L.L., von Wiren, N. and Frommer, W.B. (2007) A cytosolic *trans*-activation domain essential for ammonium uptake. Nature 446, 195–198.
[29] Britto, D.T., Glass, A.D., Kronzucker, H.J. and Siddiqi, M.Y. (2001) Cytosolic concentrations and transmembrane fluxes of NH_4^+/NH_3. An evaluation of recent proposals. Plant Physiol. 125, 523–526.
[30] Britto, D.T., Siddiqi, M.Y., Glass, A.D. and Kronzucker, H.J. (2001) Futile transmembrane NH_4^+ cycling: a cellular hypothesis to explain ammonium toxicity in plants. Proc. Natl. Acad. Sci. USA 98, 4255–4258.
[31] Guether, M., Neuhauser, B., Balestrini, R., Dynowski, M., Ludewig, U. and Bonfante, P. (2009) A mycorrhizal-specific ammonium transporter from lotus Japonicus acquires nitrogen released by Arbuscular Mycorrhizal Fungi. Plant Physiol. 150, 73–83.